

Dimensional reduction by conformal bootstrap

Shinobu Hikami*

Mathematical and Theoretical Physics Unit, Okinawa Institute of Science and Technology Graduate University, Okinawa, Onna 904-0495, Japan

*E-mail: hikami@oist.jp

Received October 29, 2018; Revised June 6, 2019; Accepted June 19, 2019; Published August 13, 2019

.....
Dimensional reductions in the branched polymer model and the random field Ising model (RFIM) are discussed by a conformal bootstrap method. Small minors are applied for the evaluations of the scale dimensions of these two models and the results are compared to the $D' = D - 2D$ Yang–Lee edge singularity and to the pure $D' = D - 2D$ Ising model, respectively. For the former case, the dimensional reduction is shown to be valid for $3 \leq D \leq 8$ and, for the latter case, the deviation from the dimensional reduction can be seen below five dimensions.
.....

Subject Index A41

1. Introduction

The critical exponent of a D -dimensional branched polymer, which is a polymer with trivalent branches in a D -dimensional solvent, is known to be same as the critical exponent of the $D'D$ Yang–Lee edge singularity with $D' = D - 2$. The dimension D has a range of $3 \leq D \leq 8$ for this correspondence. This remarkable correspondence has been explained by the supersymmetry [1] for such a dimensional range. There is also perturbational analysis near eight dimensions by ϵ expansion, which supports this dimensional reduction. This dimensional reduction has been proved rigorously for the branched polymer [3–5].

A random magnetic field Ising model (RFIM) was conjectured to have dimensional reduction to the pure Ising model without magnetic field by the supersymmetric formulation; namely, the critical exponents of RFIM in D dimensions are the same as the critical exponents of the pure Ising model in $D' = D - 2$ dimensions for $3 < D \leq 6$ [2]. This conjectured was, however, disproved by the counterexample of $D = 3$. It has been shown that there is a phase transition in $D = 3$ for RFIM [6].

The failure of the supersymmetric argument for the dimensional reduction of RFIM is related to the negative sign of the measure of the functional integral after the integration of the Grassmann fields. The instability of the fixed point in the ϵ expansion has also been discussed [7]. The formation of a bound state has been proposed [8,9]. The problem of the dimensional reduction of RFIM has persisted for 40 years. The review article [10] provides recent references for RFIM, including a numerical analysis. We will investigate RFIM in this article by the conformal bootstrap method, which has been applied to the Yang–Lee edge singularity [12–14] and for the branched polymer [15]. We will again discuss the branched polymer case to see a clear difference to RFIM by the conformal bootstrap method.

The conformal bootstrap method was developed a long time ago [16], and it was applied to critical phenomena [17,18] as an approximation. The modern numerical approach was initiated by Ref. [19]. The recent studies by this conformal bootstrap method led to many remarkable results for various symmetries, references to which may be found in a recent review article [20].

The result of the conformal bootstrap method in this article is consistent with the dimensional reductions in the case of the branched polymer and RFIM. Since our analysis is limited to the small size of the determinant of the conformal block, the result should be interpreted as an approximation for the critical exponent. This method, however, as shown in the Yang–Lee edge singularity [14], has an advantage over the standard ϵ expansion, since it estimates critical exponents in a wide region of the space dimensions, not restricted to the area near the upper critical dimensions.

For the RFIM, the result suggests that the dimensional reduction will hold near $D = 6$ up to $D = 5$, but below $D = 5$, the values of the critical exponent of D dimensions deviate from the conjecture that the dimensional reduction holds; the corresponding critical exponents in $D' = D - 2$ dimensions are the critical exponents of the Ising model.

We simply call the method that we employ in this paper a determinant method. With the restriction to small numbers of operators, the determinant method has been applied successfully to the Ising model and the Yang–Lee edge singularity [12–14]. This determinant method can be applied to non-unitary cases, since it does not require a unitarity bound. The unitary case, such as the $O(N)$ vector model ($N \geq 1$), shows a kink in the boundary curve of the unitarity bound. If we identify this kink as a critical point, we obtain the value of the critical exponent. The Yang–Lee edge singularity and $O(N)$ vector model for $N < 1$ are, however, not unitary, since the operator coefficients become negative. Disordered systems, like the branched polymer and RFIM, are described by a non-unitary model. The determinant method (or truncation method) may be useful for obtaining the critical exponents for the non-unitary models [20]. At the moment we do not know of another method for non-unitary cases.

The branched polymer and RFIM are expressed by the replica limit $N \rightarrow 0$ of the N -component Ginzburg–Landau effective action. We use a few scale dimensions Δ for the analysis for the bootstrap method instead of infinite numbers of different Δ . We consider only small values of spin L , namely $L = 2$ and $L = 4$. For the disordered system, the degeneracy of two different scalar Δ becomes essentially important. In this paper, we introduce one scalar scaling dimension Δ_1 , which is chosen as a free parameter, in addition to the basic energy scale dimension Δ_ϵ . It is known that Δ_ϵ is a scale dimension for the energy density, and is related to the critical exponent ν . The other scaling dimension Δ_1 appears as a traceless symmetric tensor scaling dimension in the $O(N)$ vector model. For the polymer case, expressed in the replica limit $N = 0$ in the $O(N)$ vector model, this scaling dimension Δ_1 coincides with the energy density scale dimension Δ_ϵ [15,23]. In the single polymer and branched polymer cases, this Δ_1 is the same as $\Delta_T = D - \hat{\phi}/\nu$, where $\hat{\phi}$ is a crossover exponent of the $O(N)$ vector model [24]. Thus the degeneracy of two scalar Δ occurs as $\Delta_T = \Delta_\epsilon$. In RFIM, we do not necessarily assume that Δ_1 is the same as Δ_T , as expected. Indeed, the effective replica Hamiltonian is different from polymers as we will see in Eq. (2). We assume the value of Δ_1 to be near the value of Δ_ϵ , similar to the polymer case, although Δ_1 is assumed to be different from the scale dimension $\Delta'_\epsilon = D + \omega$, where ω is an exponent of the correction to scaling, since Δ_1 and Δ'_ϵ are both scalar scale dimensions. There is no reason for Δ_1 to be the same as the scale dimension Δ_ϵ , when the dimensional reduction due to the supersymmetry does not hold for RFIM.

This paper is organized as follows: In Sect. 2, the Yang–Lee edge singularity is briefly reviewed as an example of the application of the determinant method. In Sect. 3 we give a brief review of the conjecture of the random magnetic field Ising model (RFIM) by the renormalization group and by the supersymmetric argument, which leads to the conclusion that RFIM is equivalent to the $D - 2D$ pure Ising model. In Sect. 4, the dimensional reduction of the branched polymer to the Yang–Lee edge singularity is explained by a supersymmetric argument similar to RFIM. In Sect. 5,

we discuss the dimensional reduction of the branched polymer to the Yang–Lee edge singularity by the determinant method. In Sect. 6, we discuss RFIM by the determinant method, and see the validity of the dimensional reduction to the pure Ising model. Section 7 is devoted to the summary and discussions. An explanation of the determinant method has been presented in Refs. [14,15]. The various related notations are also represented in them. We do not repeat these fundamental equations for brevity, and recommend that the reader consult these equations in Refs. [14,15].

2. Yang–Lee singularity in $1 \leq D \leq 6$

We first consider the Yang–Lee edge singularity [11], since the D -dimensional branched polymer has a dimensional reduction to the $D - 2$ D Yang–Lee edge singularity. The Yang–Lee edge singularity is a good example of the determinant method, which we will apply to RFIM later. It originates from the critical behavior of the density of the zeros of the partition function of the Ising model with a complex magnetic field. It is described by ϕ^3 field theory with an imaginary coupling constant. This Yang–Lee edge singularity has been studied by the conformal bootstrap method [12–14].

We consider a finite scale dimensions Δ . The four scaling dimensions, Δ_ϕ , Δ_ϵ , Δ'_ϵ , denote the scaling dimensions for a field ϕ , an energy ϵ , and a correction to scaling ω , respectively and we also include Q (a spin-4 operator, fourth derivative). The definition of these four parameters can be found in Refs. [12] and [14]. For the Yang–Lee edge singularity, which is described by ϕ^3 theory with an imaginary coefficient, the constraint of the degeneracy due to the equation of motion, $\Delta_\phi = \Delta_\epsilon$, is imposed. In the map of zero loci of 4×4 minors, there appear several intersection points of zero loci lines. In a previous article [14], we discussed the reason for the existence of such intersection points of three or more lines of the zeros of minors by the Plücker relations. Below we repeat the results for $D = 6, 4$, and 3 for the Yang–Lee edge singularity, which has been investigated in Ref. [14].

- $D = 6$

In Fig. 1, the zero loci of 4×4 minors in $D = 6$ intersect at three fixed points with parameters of $Q = 8$ and $\Delta'_\epsilon = 5.9$. The upper one is a free-field fixed point with $\Delta_\phi = 2.0$ and $\Delta_\epsilon = 4.0$, and the middle intersection point is the continuation of the non-trivial fixed point of Wilson–Fisher to six dimensions (infrared unstable). The lower fixed point corresponds to the Yang–Lee edge singularity ($\Delta_\epsilon = \Delta_\phi = 2.0$). The horizontal line at $\Delta_\epsilon = 2.0$ shows a pole of $\Delta = \frac{D-2}{2}$ for $D = 6$ [21,22].

- $D = 4$

In Fig. 2, with $D = 4$, $Q = 6.0$, and $\Delta'_\epsilon = 4.0$, the intersection points appear at (i) $\Delta_\phi = 1.0$, $\Delta_\epsilon = 2.0$, which is the Wilson–Fisher free-field point, and (ii) the Yang–Lee fixed point, which is located at $\Delta_\phi = 0.929\ 123$, $\Delta_\epsilon = 0.922\ 221$. The values of (ii) can be compared to $\Delta_\phi = 0.831\ 75$. To obtain a better value, Q is chosen as $Q = 5.712$, then the intersection point moves to $\Delta_\phi = 0.827\ 562$, $\Delta_\epsilon = 0.871\ 742$. This is close to the result by Padé analysis, which gives $\Delta_\phi = 0.831\ 75$.

- $D = 3$

The intersection map of 4×4 minors d_{ijkl} depends upon the parameters of Q and Δ'_ϵ . There is an Ising model fixed point and a Yang–Lee fixed point, but their parameters Q and Δ'_ϵ are different. When the parameters $Q = 4.75$, $\Delta'_\epsilon = 5.0$ are chosen, the Yang–Lee intersection point becomes $\Delta_\phi = 0.2314$, $\Delta_\epsilon = 0.2316$. For these parameters, the intersection point of the Ising model disappears because the parameter Q is far from the correct value ($Q = 5.02$) of the

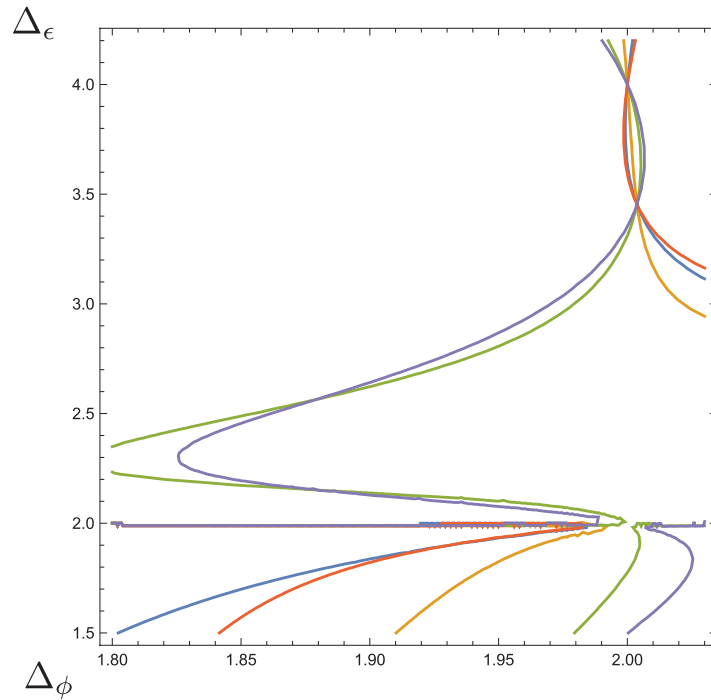


Fig. 1. $D = 6$ (Ising and Yang–Lee): The zero loci of 4×4 minors intersect at three fixed points. The upper one is the free-field fixed point $(\Delta_\phi, \Delta_\epsilon) = (2.0, 4.0)$, and the middle is the continuation of the non-trivial fixed point of Wilson–Fisher to six dimensions (infrared unstable). The lower fixed point corresponds to the Yang–Lee edge singularity $(\Delta_\epsilon = \Delta_\phi = 2.0)$.

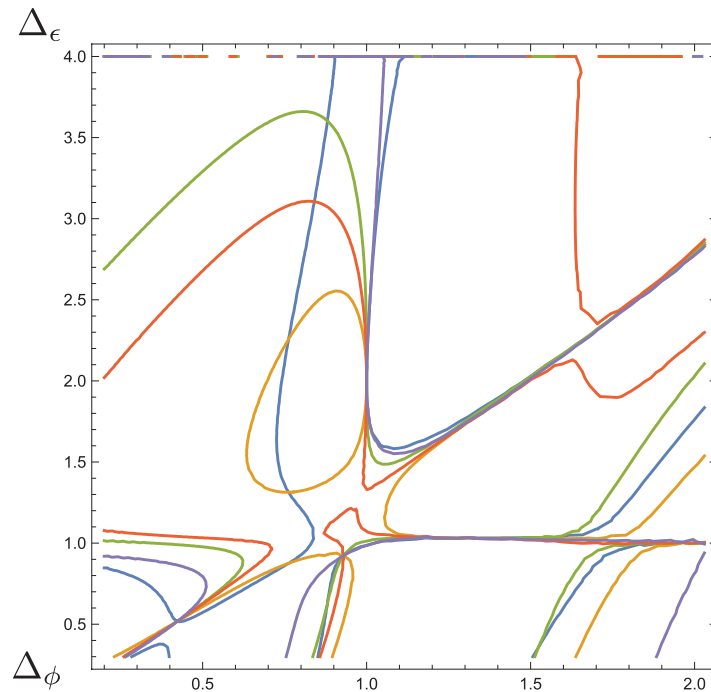


Fig. 2. Yang–Lee in $D = 4$: The zero loci of 4×4 minors intersect at three fixed points. The free-field fixed point for ϕ^4 theory at $\Delta_\phi = 1, \Delta_\epsilon = 2$ is shown as an intersection point of the five minor loci. The lower fixed point corresponds to the Yang–Lee edge singularity $(\Delta_\epsilon = \Delta_\phi = 0.8)$. The parameters $Q = 6.0$ and $\Delta_{\epsilon'} = 4.0$ are chosen.

Table 1. The scale dimensions of the Yang–Lee model [14] (* denotes exact value).

| | $\Delta_\phi = \Delta_\epsilon$ | Q | Δ_ϕ (Padé) |
|-----------|---------------------------------|----------|----------------------|
| $D = 2.0$ | -0.4^* | 3.6^* | — |
| $D = 3.0$ | 0.174 343 | 4.341 06 | 0.229 95 |
| $D = 3.5$ | 0.499 401 | 5.041 95 | 0.531 53 |
| $D = 4.0$ | 0.823 283 | 5.711 52 | 0.831 75 |
| $D = 4.5$ | 1.137 55 | 6.333 95 | 1.1300 |
| $D = 5.0$ | 1.438 07 | 6.917 16 | 1.4255 |
| $D = 5.5$ | 1.724 69 | 7.469 85 | 1.7165 |
| $D = 6.0$ | 2.0 | 8.0 | 2.0 |

Ising model. From the Padé analysis, the scale dimension $\Delta_\phi = \Delta_\epsilon$ is obtained as $\Delta_\phi = 0.2299$ [14].

The values of $\Delta_\phi = \Delta_\epsilon$, which are obtained by the determinant method in Ref. [14] are listed in general dimensions in Table 1, which will be used in the discussion of the dimensional reduction.

3. Random magnetic field Ising model (RFIM)

The dimensional reduction in the D -dimensional random magnetic field Ising model to the pure Ising model in $D - 2$ dimensions has been discussed intensively, by a diagrammatic perturbation [30] and by a supersymmetric argument [2]. Their results support the dimensional reduction to the pure Ising model in $D - 2$ dimensions. However, this dimensional reduction for RFIM was found to be incorrect. Particularly for the lower dimension, it has been proved that the lower dimension is not three [6].

There are several suggestions for the reason for this breakdown. It is recognized that RFIM is related to replica symmetry breaking like the spin glass problem due to the negative sign, since the measure expressed as a determinant by Grassmannian variables can be negative. Also it was shown that the fixed point becomes unstable on introducing more relevant couplings. [7,8].

This puzzling problem has stood for a long time from the beginning of the renormalization group study more than 40 years ago. It is known that the dimensional reduction works for (i) the branched polymer in D dimensions, which is equivalent to the Yang–Lee edge singularity in $D' = D - 2$ dimensions, and (ii) the electron density of state in a 2D random impurity potential under a strong magnetic field [28,34].

We briefly summarize in the following the argument of the dimensional reduction of RFIM. The application of the replica method to RFIM is the replacement of the following action:

$$S(\phi) = \int d^Dx \left[\frac{1}{2}(\nabla\phi)^2 + \frac{1}{2}r\phi^2 + \frac{1}{8}g\phi^4 - h(x)\phi(x) \right] \tag{1}$$

by

$$S(\phi_\alpha) = \int d^Dx \left[\sum_{\alpha=1}^N \left(\frac{1}{2}(\nabla\phi_\alpha)^2 + \frac{1}{2}t\phi_\alpha^2 + \frac{1}{8}u\phi_\alpha^4 \right) - \frac{c}{2} \sum_{\alpha,\beta=1}^N \phi_\alpha\phi_\beta \right] \tag{2}$$

with a random magnetic field $h(x)$, which obeys the white noise distribution:

$$\langle h(x) \rangle = 0, \quad \langle h(x)h(x') \rangle = c\delta(x - x'). \tag{3}$$

The quenched average requires about $W = \log Z$, and the replica $N \rightarrow 0$ limit takes this average about Z as

$$\lim_{N \rightarrow 0} \frac{1}{N} (\langle Z^N \rangle - 1) = \langle \log Z \rangle. \quad (4)$$

Under this c , the propagator G in the replica follows as

$$G^{\alpha,\beta}(q) = \frac{\delta_{\alpha\beta}}{q^2 + t} + \frac{c}{(q^2 + t)(q^2 + t - Nc)}. \quad (5)$$

The loop expansion of this propagator shows a critical dimension at $D = 6$ in the limit $N \rightarrow 0$ since the propagator changes due to the non-vanishing c , such as

$$I(p) = \int d^D q \frac{1}{(q^2 + t)(q^2 + t - Nc)((p - q)^2 + t)((p - q)^2 + t - Nc)}. \quad (6)$$

Indeed, $\epsilon = (6 - D)$ expansion gives

$$\frac{1}{\nu} = 2 - \frac{N + 2}{N + 8} \epsilon + O(\epsilon^2), \quad (7)$$

which has the same form as the ordinary $O(N)$ vector model without a random magnetic field of $\epsilon = 4 - D$.

Parisi and Sourlas [2] introduced anticommuting variables instead of the replica field, which plays with -2 dimensions, in the stochastic field formulation.

The Green's function $G(x) = \langle \phi(x)\phi(0) \rangle$ is

$$\begin{aligned} G(x) &= \int D\phi D\omega D\psi \phi(x)\phi(0) \exp\left[-\int d^D y \left(-\frac{1}{2}\omega^2 + \omega[-\Delta\phi + V'(\phi)]\right.\right. \\ &\quad \left.\left.+ \bar{\psi}[-\Delta + V''(\phi)]\psi\right)\right] \\ &= \int D\phi Dh \phi(x)\phi(0) \delta(-\Delta\phi + V'(\phi) + h) \det[-\Delta + V''(\phi)] \\ &\quad \times \exp\left[-\frac{1}{2} \int h^2(y) d^D y\right], \end{aligned} \quad (8)$$

where $V(\phi) = \frac{1}{2}m^2\phi^2 + g\phi^4$. The shortcoming of this formulation is the sign of the determinant, which can be negative. There appears a supersymmetric BRST gauge transformation [33],

$$\begin{aligned} \delta\phi &= -\bar{a}\epsilon_\mu x_\mu \psi, \quad \delta\omega = 2\bar{a}\epsilon_\mu \partial_\mu \psi, \\ \delta\psi &= 0, \quad \delta\bar{\psi} = \bar{a}(\epsilon_\mu x_\mu \omega + 2\epsilon_\mu \partial_\mu \phi), \end{aligned} \quad (9)$$

where \bar{a} is an infinitesimal anticommuting number and ϵ_μ is an arbitrary vector. With the superfield $\Phi(x, \theta)$,

$$\Phi(x, \theta) = \phi(x) + \bar{\theta}\psi(x) + \bar{\psi}(x)\theta + \theta\bar{\theta}\omega(x), \quad (10)$$

the Lagrangian becomes

$$L(\Phi) = -\frac{1}{2}\Phi\Delta_{ss}\Phi + V(\Phi) \quad (11)$$

with $\Delta_{ss} = \Delta + \partial^2 / \partial \bar{\theta} \partial \theta$. The superspace (x, θ) is equivalent to $D - 2$ dimensional space. Therefore, the anticommuting coordinate has a negative dimension -2 . This may give a possible proof of the dimensional reduction from D to $D - 2$, but as we discussed before, this dimensional reduction does not work, since the measure does not show the positivity.

4. Branched polymer

We briefly consider the branched polymer since the formulation is very close to RFIM. The main difference is that the effective Hamiltonian is ϕ^3 instead of ϕ^4 for the branched polymer. This makes the upper critical dimension eight for the branched polymer. (RFIM has an upper critical dimension of six). The branched polymer is described by branching terms in addition to the self-avoiding term. We write the action for a p th branched polymer as N -replicated field theory:

$$S = \int d^D x \left(\frac{1}{2} \sum_{\alpha=1}^N ((\nabla \phi_\alpha)^2 - \sum_{p=1}^{\infty} u_p \phi_\alpha^p) + \lambda \left(\sum_{\alpha=1}^N \phi_\alpha^2 \right)^2 \right). \quad (12)$$

The term ϕ_α^p represents the p th branched polymer. After rescaling and neglecting irrelevant terms, the following action is obtained:

$$S = \int d^D x \left(\frac{1}{2} \sum_{\alpha=1}^N ((\nabla \phi_\alpha)^2 + V(\phi_\alpha)) + C \sum_{\alpha, \beta=1}^N \phi_\alpha \phi_\beta \right) \quad (13)$$

with $V(\phi_\alpha) = t\phi_\alpha - \frac{1}{3}\phi_\alpha^3 + O(\phi_\alpha^4)$.

In the paper of Parisi–Sourlas [1], the equivalence to the Yang–Lee edge singularity was shown by the supersymmetric argument. The ϵ expansion of the critical exponent η of the branched polymer was studied [11,27]:

$$\eta = -\frac{1}{9}\epsilon, \quad (14)$$

where $\epsilon = 8 - D$. The scaling dimension Δ_ϕ becomes

$$\Delta_\phi = \frac{D - 2 + \eta}{2}. \quad (15)$$

In this formula, we put $D \rightarrow D - 2$, and $\epsilon \rightarrow \epsilon = 6 - D$, then we get

$$\Delta_\phi = 2 - \frac{5}{9}\epsilon, \quad (16)$$

where $\epsilon = 6 - D$. This last formula is exactly the same as the expansion of the Yang–Lee edge singularity, $\Delta_\phi = 2 - \frac{5}{9}\epsilon$, with $\epsilon = 6 - D$.

The exponent ν of the Yang–Lee edge singularity ($\epsilon = 6 - D$) is

$$\frac{1}{\nu} = \frac{1}{2}(D + 2 - \eta) = \frac{1}{2}(8 - \epsilon + \frac{1}{9}\epsilon) = 4 - \frac{4}{9}\epsilon. \quad (17)$$

This reads, up to order ϵ ,

$$\Delta_\epsilon = D - \frac{1}{\nu} = (6 - \epsilon) - (4 - \frac{4}{9}\epsilon) = 2 - \frac{5}{9}\epsilon = \Delta_\phi. \quad (18)$$

Table 2. The branched polymer in D dimensions. $\Delta_\phi = 3(D - 3)/5$ (approximation) and (A) the scale dimension of the Yang–Lee model in $D' = D - 2$ dimensions obtained from Eq. (22), (B) the scale dimension of the Yang–Lee model in $D' = D - 2$ dimensions obtained from the Padé or exact solution (*).

| D | Δ_ϕ (branched polymer) $= 3(D - 3)/5$ | $D' = D - 2$ | (A) Δ_ϕ (Yang–Lee edge singularity) | (B) Δ_ϕ (Yang–Lee edge singularity) |
|-----------|--|--------------|--|--|
| $D = 3.0$ | 0.0 | $D' = 1.0$ | −1.0 | −1.0* |
| $D = 4.0$ | 0.6 | $D' = 2.0$ | −0.4 | −0.4* |
| $D = 5.0$ | 1.2 | $D' = 3.0$ | 0.2 | 0.23 |
| $D = 6.0$ | 1.8 | $D' = 4.0$ | 0.8 | 0.83 |
| $D = 7.0$ | 2.4 | $D' = 5.0$ | 1.4 | 1.43 |
| $D = 8.0$ | 3.0 | $D' = 6.0$ | 2.0 | 2.0* |

Thus the values of the exponents η and ν of the branched polymer become the same as the exponents of the Yang–Lee edge singularity. This holds for all orders of ϵ due to the equation of motion. The scale dimensions of Δ_ϵ and Δ_ϕ , however, become different since they involve the space dimension D explicitly. For instance, in the branched polymer at $D = 8$,

$$\Delta_\epsilon = 8 - \frac{1}{\nu} = 4, \quad \Delta_\phi = 3, \quad (19)$$

where, for the Yang–Lee edge singularity at $D = 6$,

$$\Delta_\epsilon = 2, \quad \Delta_\phi = 2. \quad (20)$$

In the general dimension $D \leq 8$, from the relation to the Yang–Lee edge singularity, we have, for the branched polymer,

$$\Delta_\epsilon = \Delta_\phi + 1, \quad (21)$$

as shown in Eq. (19) for $D = 8$. We get the following relations by noting the difference of the dimension D for the two cases:

$$\begin{aligned} \Delta_\phi(\text{branched polymer in } D \text{ dim.}) &= \Delta_\phi(\text{Yang–Lee in } D' \text{ dim.}) + 1, \\ \Delta_\epsilon(\text{branched polymer in } D \text{ dim.}) &= \Delta_\epsilon(\text{Yang–Lee in } D' \text{ dim.}) + 2, \end{aligned} \quad (22)$$

where $D' = D - 2$. This relation is related to the $\mathcal{N} = 1$ supersymmetric Ising model, which has been pointed out in Refs. [23,35,36].

5. Conformal bootstrap for the branched polymer

We now consider the determinant method for the branched polymer. This determinant method will be applied to the RFIM in the next section.

The minor d_{123} is defined by

$$d_{123} = \det \begin{pmatrix} vs1 & vs2 & vs3 \\ vs1' & vs2' & vs3' \\ vt1 & vt2 & vt3 \end{pmatrix}, \quad (23)$$

Table 3. Expected correspondence for RFIM to the $D' = D - 2D$ Ising model.

| D | Δ_ϕ (RFIM) | Δ_ϵ (RFIM) | $D' = D - 2$ | Δ_ϕ (Ising) | Δ_ϵ (Ising) |
|---------|----------------------|--------------------------|--------------|-----------------------|---------------------------|
| $D = 6$ | 2.0 | 4.0 | $D' = 4$ | 1.0 | 2.0 |
| $D = 5$ | 1.516 | 3.414 | $D' = 3$ | 0.516 | 1.414 |
| $D = 4$ | 1.125 | 3.0 | $D' = 2$ | 0.125 | 1.0 |

where $vs_n = vs_n(D, \Delta_\phi, \Delta_\epsilon)$ ($n = 1, 2, 3$). The number n is related to the derivative of the conformal block. The notation of vs_n can be found in Ref. [14]. vs_n' is a function of D , Δ_ϕ , and Δ_1 . Δ_1 represents the scalar scale dimension Δ_T , which appears in the polymer case [15,23].

For a polymer, which is represented in the limit $N \rightarrow 0$ in the $O(N)$ vector model, the conformal bootstrap method was applied with the $O(N)$ symmetric tensor scale dimension Δ_T , which becomes equal to Δ_ϵ [15]. The $O(N)$ symmetric tensor field $\phi_{ab}(x)$ is given by

$$\phi_{ab}(x) =: \phi_a \phi_b : - \frac{\delta_{ab}}{N} \sum_{m=1}^N : \phi_m^2 : \tag{24}$$

and the energy density $\epsilon(x)$ is defined by

$$\epsilon(x) = \sum_{m=1}^N : \phi_m^2 : . \tag{25}$$

The crossover exponent of the $O(N)$ vector model $\hat{\phi}_2$ is given as

$$\hat{\phi} = \frac{D - \Delta_T}{D - \Delta_\epsilon} \tag{26}$$

and for a polymer ($N=0$), $\hat{\phi}$ becomes 1, and it leads to the degeneracy of $\Delta_T = \Delta_\epsilon$ [23]. The determinant method for the polymer with the scaling dimension Δ_T provides good numerical values for the critical exponents [15].

For a branched polymer, which is represented by the bosonic Hamiltonian in Eq. (13), the $O(N)$ symmetric tensor scale dimension Δ_T is also important. This scale dimension is a scalar, and we denote this for the branched polymer by Δ_1 in the following.

We put $\Delta_\phi = 3(D - 3)/5$ as an approximation value for the branched polymer, which is not so different from the expected value in Table 3, and we determine the value of Δ_ϵ and Δ_1 ($\Delta_1 = \Delta_T$) from the intersection of the zero loci of 3×3 minors d_{ijk} . In Fig. 3, we consider $D = 8$. The intersection point shows $\Delta_\epsilon = \Delta_1 = 4$. In Fig. 4, $D = 6$ is shown. In Fig. 5, the $D = 4$ case is shown with $\Delta_\phi = 0.6$. The obtained value $\Delta_\epsilon = 1.6$ is consistent with the Yang–Lee edge singularity at $D = 2$, $\Delta_\phi = \Delta_\epsilon = -0.4$. Thus we find that, as in Figs. 3– 5, the dimensional reduction to the $D' = D - 2D$ Yang–Lee edge singularity holds.

For the 4×4 minor method, the four scale dimensions are Δ_ϕ , Δ_ϵ , Δ_1 , and Q . Q is the spin-4 scale dimension. For the polymer case, $\Delta_T = \Delta_\epsilon$, but for the Ising model Δ_T is not equal to Δ_ϵ . It takes a value near Δ_ϵ [23].

◦ $D = 6$

The fixed point at $\Delta_\phi = 1.8$ and $\Delta_\epsilon = 2.8$ is obtained for $D = 6$. These scale dimensions are consistent with the dimensional reduction to $D' = 4$ ($D' = D - 2$)D Yang–Lee edge singularity. This case is represented in Fig. 3 of Ref. [15].

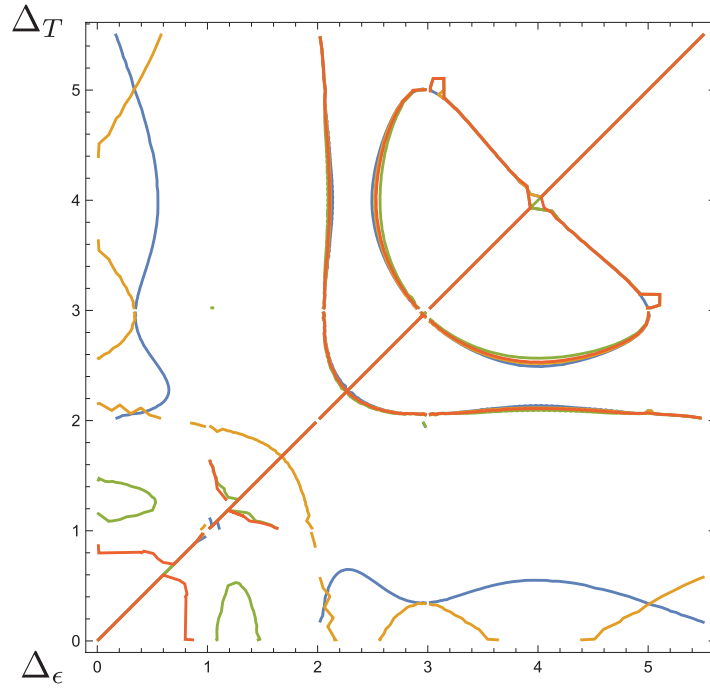


Fig. 3. Branched polymer of $D = 8.0$, $\Delta_\phi = 2.0$: the contours of zero loci of 3×3 minors d_{124} , d_{123} , d_{234} , d_{134} are shown. At $\Delta_\epsilon = 4.0$, the fixed point appears for a branched polymer.

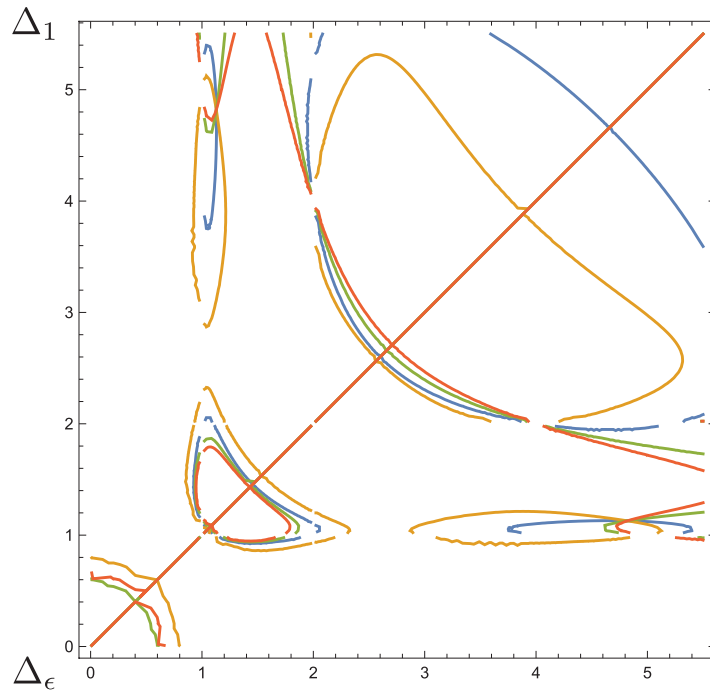


Fig. 4. Branched polymer of $D = 6$. Four lines, the contours of zero loci of d_{124} , d_{123} , d_{234} , d_{134} , intersect with the line $\Delta_\epsilon = \Delta_1 (= \Delta_T)$ at $\Delta_\epsilon = 2.8$, which corresponds to the Yang–Lee model at $D = 4$ in Table 1. In this figure, $\Delta_\phi = 0.83$ is taken.

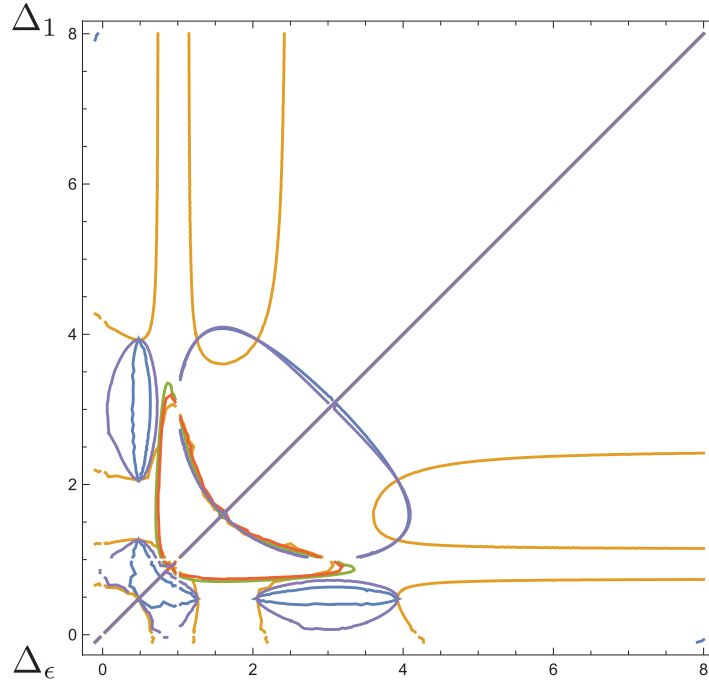


Fig. 5. Branched polymer of $D = 4$. 3×3 determinant method with $\Delta_\phi = 0.6$: the contours of zero loci of $d_{124}, d_{123}, d_{234}, d_{134}, d_{125}$ are shown. The fixed point is obtained at $\Delta_\epsilon = \Delta_1 = 1.6$ from the intersection of five lines of the zero loci. The correspondence of $\Delta_\epsilon = 1.6 - 2 = -0.4$ to the exact value of the Yang–Lee edge singularity at $D = 2$ is verified. The axis is $(x, y) = (\Delta_\epsilon, \Delta_1)$. This figure shows an enlargement of the singularity of $\Delta_\epsilon = \Delta_1$ to $\Delta_\epsilon \neq \Delta_1$. There is another fixed point at $\Delta_1 = 3.3$, which is considered as the correction to scaling Δ'_ϵ .

◦ $D = 5$

For $D = 5$, we find in Fig. 6 a fixed point of $\Delta_\phi = 1.25, \Delta_\epsilon = 2.4$ for the branched polymer. These scale dimensions are consistent with the dimensional reduction to the Yang–Lee edge singularity of $D' = 3$ dimensions ($D' = D - 2$). We used the parameters of $Q = 7.0, \Delta_1 = 2.6$ in Fig. 6.

6. Conformal bootstrap for RFIM

The relations between the scale dimension Δ_ϕ and Δ_ϵ of RFIM and the pure Ising model are, if they hold,

$$\Delta_\phi(\text{RFIM in } D \text{ dim.}) = \Delta_\phi(\text{pure Ising in } D' \text{ dim.}) + 1 \tag{27}$$

and

$$\Delta_\epsilon(\text{RFIM in } D \text{ dim.}) = \Delta_\epsilon(\text{pure Ising in } D' \text{ dim.}) + 2, \tag{28}$$

where $D' = D - 2$.

There are several arguments that explain the failure of the above dimensional reduction of RFIM. The most serious argument against the dimensional reduction may be the existence of the attractive potential of replica fields, which leads to the bound states [8,9]. Recently, the breakdown of the

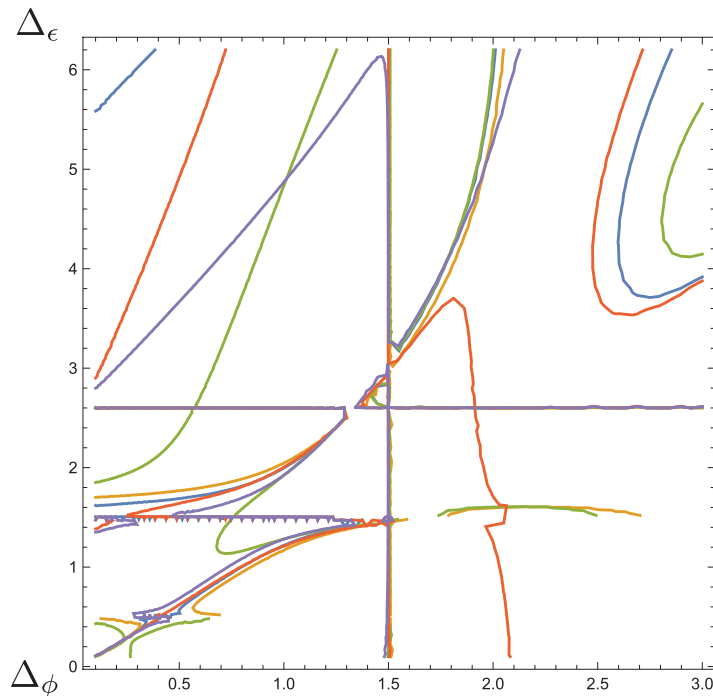


Fig. 6. Branched polymer in $D = 5$: the contours of zero loci of minors are shown. The fixed point $\Delta_\epsilon = 2.45$, $\Delta_\phi = 1.25$ is obtained with $\Delta_1 = 2.6$, $Q = 7.0$. This corresponds to the $D' = 3$ Yang–Lee edge singularity $\Delta_\epsilon = \Delta_\phi = 0.23$ in Table 2.

dimensional reduction has been suggested near $D = 5$ [31]. A recent review of RFIM may be found in Refs. [10,32].

Assuming that this dimensional reduction works near six dimensions for the random field Ising model, the conformal bootstrap method may be applied numerically for RFIM. From the dimensional reduction, we expect the correspondence of Table 3.

In Fig. 7 and $D = 6$, $\Delta_1 = 4.9$, we have a single fixed point at $\Delta_\phi = 2$, $\Delta_\epsilon = 4$, which agrees with the $D = 4$ Ising fixed point by dimensional reduction. We examine the fixed points around $D = 6$. By another analysis, where a parameter $\Delta_1 = 4.3$ is chosen, we have the same result. These values exactly correspond to the $D = 4$ pure Ising model at $D = 4$. Namely, the dimensional reduction of RFIM is valid for $D = 6$. We note that the value of Δ_1 is slightly different from Δ_ϵ .

In Fig. 8, the $D = 5.9$ case with $\Delta_1 = 4.21$, $Q = 7.9$ is shown in the contour of the zero loci of five minors. The fixed point is located at $\Delta_\epsilon = 3.933$, $\Delta_\phi = 1.94997$, which corresponds to the $D = 3.9$ pure Ising model by dimensional reduction. In Fig. 10, there is a Gaussian fixed point at $\Delta_\epsilon = D - 2 = 3.9$, which is infrared unstable. The value of Δ_ϕ is almost the same as $(D - 2)/2$, but slightly less than this value. This means that the exponent η is negative.

In Fig. 9, the $D = 5.8$ case with $\Delta_1 = 4.11$, $Q = 7.8$ is shown. The obtained values are $\Delta_\epsilon = 3.864$, $\Delta_\phi = 1.89996$. This agrees with the dimensional reduction of the pure Ising model at $D = 3.8$ by the ϵ expansion, which gives $\Delta_\epsilon = 1.8645$.

In Fig. 10, the $D = 5.0$ case with $\Delta_1 = 3.18$, $Q = 7.0$ is shown in the contour of the zero loci of five minors. The fixed point at $\Delta_\epsilon = 3.41$, $\Delta_\phi = 1.49994$ is obtained. This corresponds to the pure $D = 3.0$ Ising model ($\Delta_\epsilon = 1.414$, $\Delta_\phi = 0.516$). The value of Δ_ϵ of the pure $D = 3$ Ising model is 1.414; therefore $\Delta_\epsilon = 3.41$ agrees with the dimensional reduction, but the value of Δ_ϕ disagrees.

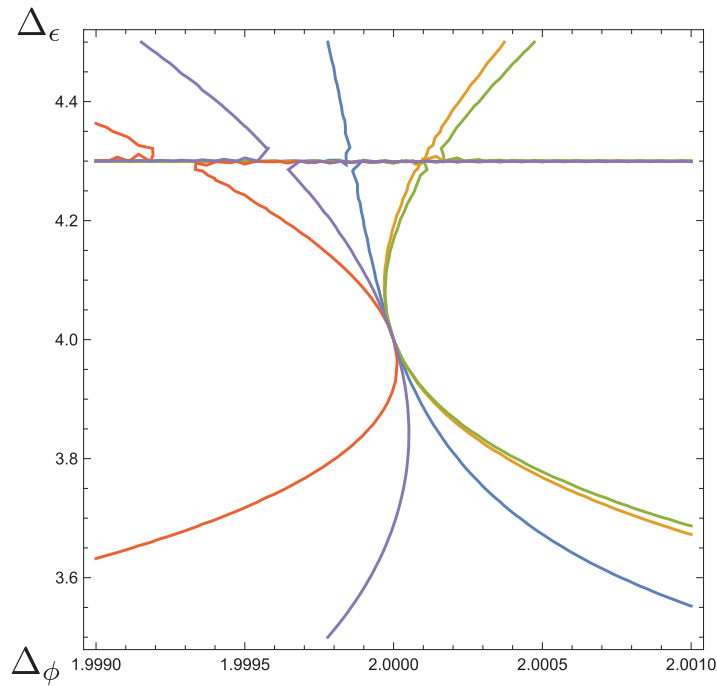


Fig. 7. RFIM in $D = 6.0$: the five contours of zero loci of 4×4 minors d_{1234} , d_{1245} , d_{2345} , d_{1245} , d_{1235} are shown with $Q = 8.0$, $\Delta_1 = 4.3$. The fixed point $\Delta_\epsilon = 4.0$, $\Delta_\phi = 2.0$ is obtained.

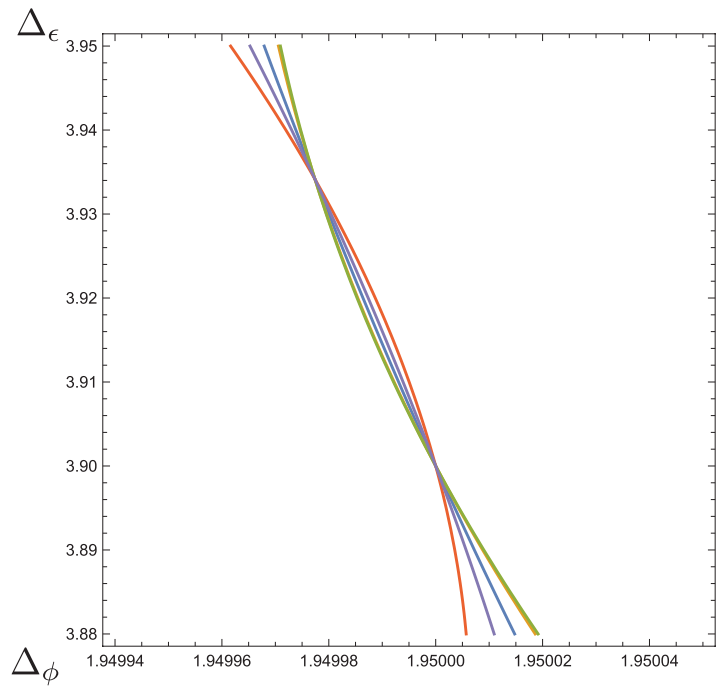


Fig. 8. $D = 5.9$: the contour of zero loci minors are shown with $Q = 7.9$, $\Delta_1 = 4.21$. The fixed point $\Delta_\epsilon = 3.933$, $\Delta_\phi = 1.94997$ is obtained.

The value of $\Delta_\phi = 1.49994$ corresponds to $\eta/2 = -0.00006$. If the value of Q is changed to 7.04, the loci of minors do not intersect in a point, although the value of Δ_ϕ approaches the dimensional reduction of the pure Ising model $\Delta_\phi = 1.514$.

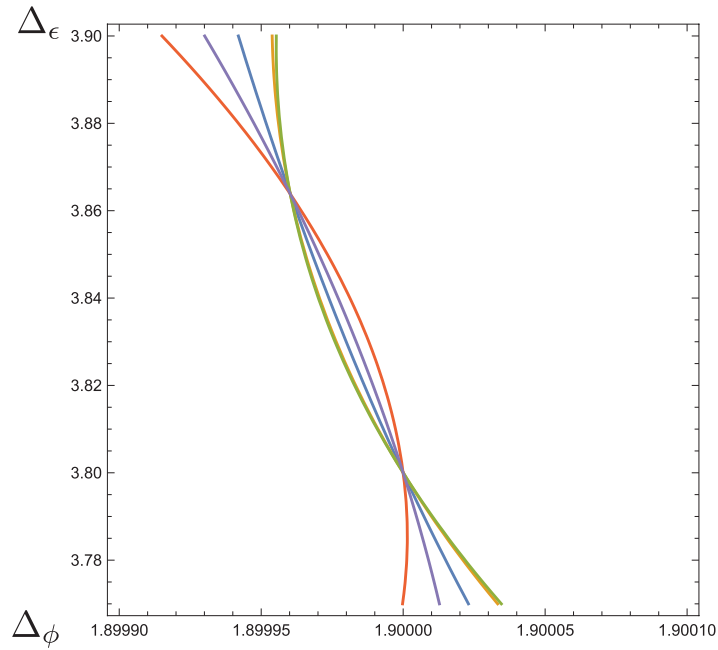


Fig. 9. $D = 5.8$: the contour of zero loci minors are shown with $Q = 7.8$, $\Delta_1 = 4.11$. The fixed point $\Delta_\epsilon = 3.864$, $\Delta_\phi = 1.89996$ is obtained.

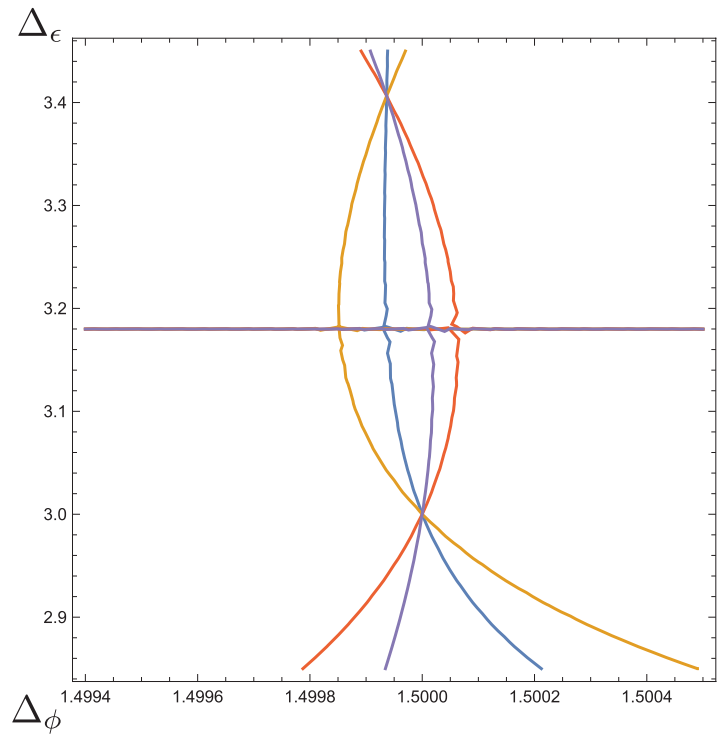


Fig. 10. $D = 5.0$: the contours of zero loci minors are shown with $Q = 7.0$, $\Delta_1 = 3.18$. The fixed point $\Delta_\epsilon = 3.41$, $\Delta_\phi = 1.49994$ is obtained.

For the $D = 4.5$ case with $\Delta_1 = 2.7$, $Q = 6.5$, the fixed point at $\Delta_\epsilon = 2.93$, $\Delta_\phi = 1.2502$ is obtained. For the $D = 4.2$ case with $\Delta_1 = 2.4$, $Q = 6.2$, the fixed point is located at $\Delta_\phi = 1.10$ and $\Delta_\epsilon = 2.55$. As shown in Table 4, the deviation of the value of Δ_ϵ from the expected value by the Padé value, which is 3.0886, is large.

Table 4. The scaling dimensions Δ_ϵ and Δ_ϕ . The values Δ_ϵ and Δ_ϕ are obtained by the 4×4 minors for values of Δ_1 and Q . These results are obtained from the analysis in Figs. 7–13. The last column is ϵ expansion in $[1, 1]$ Padé up to the second order of ϵ ($\Delta_\epsilon = 2 - 2\epsilon/3 + 19\epsilon^2/162 = (2 - 17/54\epsilon)/(1 + 19/108\epsilon)$). The value * is from Ref. [38], and the value ** is the exact value of the 2D Ising model. The values of Δ_ϵ in the fourth column agree well with the values of the sixth column for the pure Ising model in $D' = D - 2$ dimensions, when $D \geq 5$.

| D | Δ_1 | Q | Δ_ϵ | Δ_ϕ | Δ_ϵ (pure Ising in D' dim.)+ 2 |
|-----------|------------|-----|-------------------|---------------|--|
| $D = 6.0$ | 4.3 | 8.0 | 4.0 | 2.0 | 4.0 |
| $D = 5.9$ | 4.21 | 7.9 | 3.933 | 1.949 97 | 3.9345 |
| $D = 5.8$ | 4.11 | 7.8 | 3.864 | 1.899 96 | 3.8712 |
| $D = 5.5$ | 3.81 | 7.5 | 3.647 | 1.749 95 | 3.6936 |
| $D = 5.0$ | 3.18 | 7.0 | 3.41 | 1.499 94 | 3.4331(3.412 67*) |
| $D = 4.5$ | 2.7 | 6.5 | 2.93 | 1.25 | 3.2088 |
| $D = 4.2$ | 2.4 | 6.2 | 2.55 | 1.10 | 3.0886 |
| $D = 4.0$ | 2.2 | 6.0 | 2.0 | 1.0 | 3.0137(3.0**) |

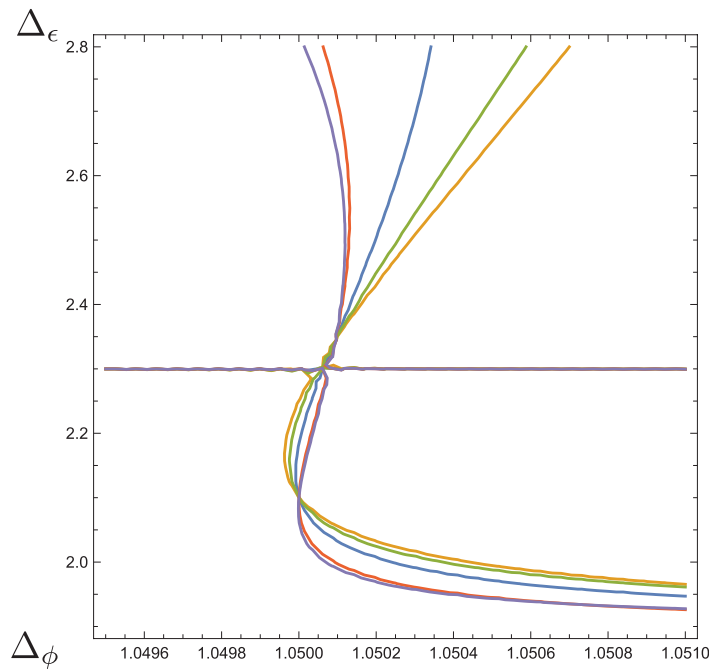


Fig. 11. $D = 4.1$: the contours of zero loci of minors are shown with $Q = 6.1$, $\Delta_1 = 2.3$. The fixed point $\Delta_\epsilon = 2.3$, $\Delta_\phi = 1.05$ is obtained.

In Fig. 11, the $D = 4.1$ case is shown with $\Delta_1 = 2.3$, $Q = 6.1$. The fixed point $\Delta_\epsilon = 2.3$, $\Delta_\phi = 1.05$ is obtained.

In Figs. 12 and 13, the $D = 4.0$ case is shown with $\Delta_1 = 2.2$, $Q = 6.0$. The fixed point $\Delta_\epsilon = 2.0$, $\Delta_\phi = 1.0$ is obtained; this is a Gaussian fixed point. Figure 13 is a global map. It is remarkable that we obtain the free-field fixed point at $D = 4$. This is due to the small value of Δ_1 . When we take a large value of Δ_1 , there appears an ordinary Ising fixed point. Indeed, when $D = 3.9$, for the larger value of $\Delta_1 = 4.0$, $Q = 5.9$, we obtain an Ising fixed point at $\Delta_\epsilon = 1.926 66$, $\Delta_\phi = 0.950 03$.

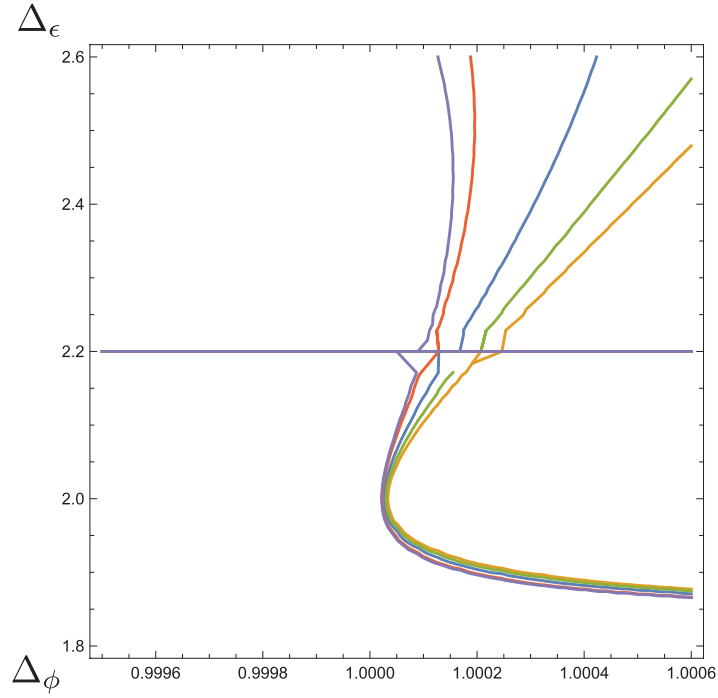


Fig. 12. $D = 4.0$: the contours of zero loci of minors are shown with $Q = 6.0$, $\Delta_1 = 2.2$. The fixed point (Gaussian) $\Delta_\epsilon = 2.0$, $\Delta_\phi = 1.0$ is obtained.

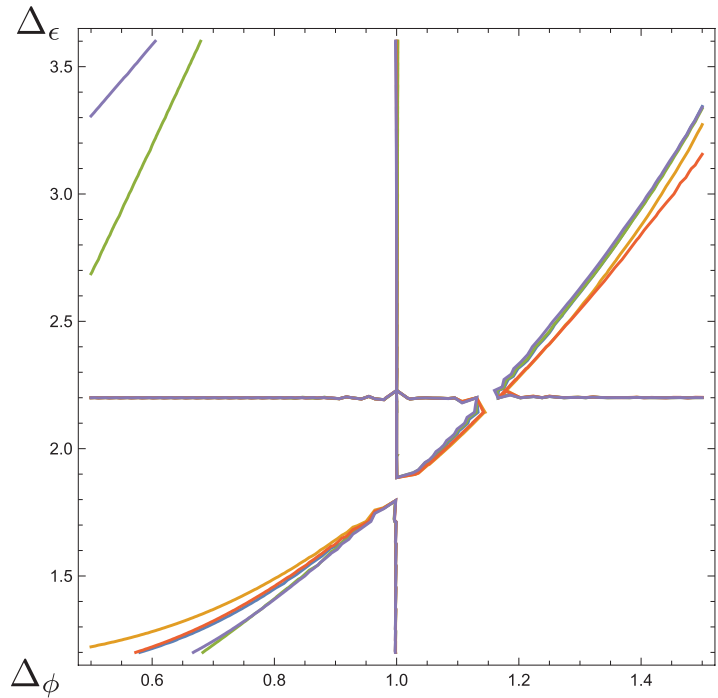


Fig. 13. $D = 4.0$ (global map): the contours of zero loci of minors are shown with $Q = 6.0$, $\Delta_1 = 2.2$. The fixed point (Gaussian) $\Delta_\epsilon = 2.0$, $\Delta_\phi = 1.0$ is on the line $\Delta_\phi = 1.0$.

AQ7

7. Summary and discussions

We have discussed in this paper the conjectures of the dimensional reductions of the branched polymer to the Yang–Lee edge singularity and RFIM to the pure Ising model by small 4×4 minors. The conformal bootstrap determinant method gives confirmations of the dimensional reductions in the branched polymer within the numerical approximations. The critical dimension of a branched polymer is 8, and it corresponds to the $D' = 6D$ Yang–Lee edge singularity. We have confirmed that, for $4 < D < 8$, there is a fixed point, which is $\Delta_\epsilon = \Delta_\epsilon$ (Yang–Lee in $D' = D - 2$ dimensions) + 2, $\Delta_\phi = \Delta_\phi$ (Yang–Lee in $D' = D - 2$ dimensions) + 1. With the relation of the Yang–Lee edge singularity model $\Delta_\epsilon = \Delta_\phi$, we obtain

$$\Delta_\epsilon = \Delta_\phi + 1, \quad (29)$$

which is a relation appearing for the $\mathcal{N} = 1$ supersymmetric Ising model [23,35,36]. These results are reported in the previous paper [15].

For RFIM, the upper critical dimension is 6. For $D < 6$, there appears a fixed point, which agrees with the values of ϵ expansion of Δ_ϵ , but the value of η becomes negatively small for $D < 6$. This result is summarized in Table 4. For $5 < D < 6$, the values of Δ_ϵ are almost consistent with the ϵ expansion, with appropriate values of Q and Δ_1 . However, for $D < 5$ the deviation becomes quite large, and the conjecture of the correspondence of the dimensional reduction is violated for $D < 5$, as seen in Table 4.

The bound state has been suggested in the literature [8,9] for the explanation of this failure of the dimensional reduction. The peculiar almost straight line as shown in Figs. 8 and 9 may indicate the bound state (also related to the negative small value of η). This finding may be consistent with the formation of the bound state. The breakdown for $D < 5$ seems to be consistent with the recent results of Refs. [10,31]. Recent work [10] also shows that the dimensional reduction of RFIM in $D = 5$ to the pure Ising model in $D' = 3$ works precisely. From the point of view of supersymmetry, we observed the difference between the Ising tri-critical point (ϕ^6 theory) and the $\mathcal{N} = 1$ supersymmetric fixed point [23], although it is well known that, in two dimensions, the tri-critical point coincides with the supersymmetric point [37]. It is interesting to investigate the relation of RFIM to multi-critical behaviors such as the tri-critical Ising model for $D < 5$. For such studies, we need more scale dimensions of the operator product expansion (OPE) in addition to the dimension Δ_1 studied here.

The random field for the $O(N)$ vector model also gives the dimensional reduction as Eq. (7). We have considered only RFIM, which is $N = 1$ of the $O(N)$ vector model. It may be important to investigate the conformal bootstrap analysis for the $O(N)$ vector spin model with the random field model. This study will be left for future work. As a disordered system, there is a problem of Anderson localization with the spin–orbit interaction [39], which has a phase transition in two dimensions. This is related to the replica limit and supersymmetry. We discuss this problem in Ref. [40].

Acknowledgements

The author is grateful to Ferdinando Gliozzi for discussions on the determinant method. He thanks Edouard Brézin for discussions on the dimensional reduction problem in branched polymers and the suggestion of the RFIM problem by the conformal bootstrap method. Part of this work was presented at the BMFT workshop at Rome University on 3 January 2018 and the author thanks Georgi Parisi for this invitation. This work is

supported by the Japan Society for the Promotion of Science (JSPS) KAKENHI Grant-in-Aid 16K05491 and 19H01813.

References

- [1] G. Parisi and N. Sourlas, Phys. Rev. Lett. **46**, 871 (1981).
- [2] G. Parisi and N. Sourlas, Phys. Rev. Lett. **43**, 744 (1979).
- [3] D. C. Brydges and J. Z. Imbrie, Ann. Math. **158**, 1019 (2003).
- [4] J. Cardy, J. Phys. A: Math. Gen. **34**, L665 (2001).
- [5] J. Cardy, [arXiv:cond-mat/0302495](https://arxiv.org/abs/cond-mat/0302495) [cond-mat.stat-mech].
- [6] J. Z. Imbrie, Phys. Rev. Lett. **53**, 1747 (1984).
- [7] E. Brézin and C. De Dominicis, EPL **44**, 13 (1998) [[arXiv:cond-mat/9804266](https://arxiv.org/abs/cond-mat/9804266)] [[Search INSPIRE](#)].
- [8] E. Brézin and C. De Dominicis, Eur. Phys. J. B **19**, 467 (2001) [[arXiv:cond-mat/0007457](https://arxiv.org/abs/cond-mat/0007457)].
- [9] G. Parisi and N. Sourlas, Phys. Rev. Lett. **89**, 257204 (2002).
- [10] N. G. Fytas, V. Martín-Mayor, M. Picco, and N. Sourlas, J. Stat. Phys. **172**, 665 (2018) [[arXiv:1711.09597](https://arxiv.org/abs/1711.09597)] [cond-mat.dis-nn] [[Search INSPIRE](#)].
- [11] M. E. Fisher, Phys. Rev. Lett. **40**, 1610 (1978).
- [12] F. Gliozzi, Phys. Rev. Lett. **111**, 161602 (2013) [[arXiv:1307.3111](https://arxiv.org/abs/1307.3111)] [hep-th] [[Search INSPIRE](#)].
- [13] F. Gliozzi and A. Rago, J. High Energy Phys. **1410**, 042 (2014).
- [14] S. Hikami, Prog. Theor. Exp. Phys. **2018**, 053I01 (2018) [[arXiv:1707.04813](https://arxiv.org/abs/1707.04813)] [hep-th] [[Search INSPIRE](#)].
- [15] S. Hikami, Prog. Theor. Exp. Phys. **2018**, 123I01 (2018) [[arXiv:1708.03072](https://arxiv.org/abs/1708.03072)] [hep-th] [[Search INSPIRE](#)].
- [16] S. Ferrara, A. F. Grillo, and R. Gatto, Ann. Phys. **76**, 161 (1973).
- [17] G. Parisi and L. Peliti, Lett. Nuovo Cimento **2**, 627 (1971).
- [18] K. Symanzik, Lett. Nuovo Cimento **3**, 734 (1972).
- [19] R. Rattazzi, V. S. Rychkov, E. Tonni, and A. Vichi, J. High Energy Phys. **0812**, 031 (2008) [[arXiv:0807.0004](https://arxiv.org/abs/0807.0004)] [hep-th] [[Search INSPIRE](#)].
- [20] D. Poland, S. Rychkov, and A. Vichi, Rev. Mod. Phys. **91**, 015002 (2019) [[arXiv:1805.04405](https://arxiv.org/abs/1805.04405)] [hep-th] [[Search INSPIRE](#)].
- [21] F. Kos, D. Poland, D. Simmons-Duffin, and A. Vichi, J. High Energy Phys. **1511**, 106 (2015) [[arXiv:1504.07997](https://arxiv.org/abs/1504.07997)] [hep-th] [[Search INSPIRE](#)].
- [22] F. Kos, D. Poland, D. Simmons-Duffin, and A. Vichi, J. High Energy Phys. **1608**, 036 (2016) [[arXiv:1603.04436](https://arxiv.org/abs/1603.04436)] [hep-th] [[Search INSPIRE](#)].
- [23] H. Shimada and S. Hikami, J. Stat. Phys. **165**, 1006 (2016).
- [24] S. Hikami and R. Abe, Prog. Theor. Phys. **52**, 369 (1974).
- [25] P.-G. de Gennes, *Scaling Concepts in Polymer Physics* (Cornell University Press, Ithaca, NY, 1979).
- [26] K. G. Wilson and M. E. Fisher, Phys. Rev. Lett. **28**, 240 (1972).
- [27] T. C. Lubensky and J. Isaacson, Phys. Rev. A **20**, 2130 (1979).
- [28] E. Brezin, D. Gross, and C. Itzykson, Nucl. Phys. B **235**, 24 (1984).
- [29] B. Duplantier and H. Saleur, Phys. Rev. Lett. **59**, 539 (1987).
- [30] Y. Imry and S.-k. Ma, Phys. Rev. Lett. **35**, 1399 (1975).
- [31] M. Tissier and G. Tarjus, Phys. Rev. Lett. **107**, 041601 (2011).
- [32] V. S. Dotsenko, J. Stat. Mech. **2007**, P09005 (2007).
- [33] A. Neveu and P. West, Phys. Lett. **182**, 343 (1986).
- [34] F. Wegner, *Supermathematics and its Applications in Statistical Physics* (Springer, Berlin, 2015), Lecture Notes in Physics Vol. 920.
- [35] L. Fei, S. Giombi, I. R. Klebanov, and G. Tarnopolsky, Prog. Theor. Exp. Phys. **2016**, 12C105 (2016).
- [36] D. Bashkirov, [arXiv:1310.8255](https://arxiv.org/abs/1310.8255) [hep-th] [[Search INSPIRE](#)].
- [37] D. Friedan, Z. Qiu, and S. Shenker, Phys. Rev. Lett. **52**, 1575 (1984).
- [38] S. El-Showk, M. F. Paulos, D. Poland, S. Rychkov, D. Simmons-Duffin, and A. Vichi, J. Stat. Phys. **157**, 869 (2014) [[arXiv:1403.4545](https://arxiv.org/abs/1403.4545)] [hep-th] [[Search INSPIRE](#)].
- [39] S. Hikami, A. I. Larkin, and Y. Nagaoka, Prog. Theor. Phys. **63**, 707 (1980).
- [40] S. Hikami, [arXiv:1811.05918](https://arxiv.org/abs/1811.05918) [cond-mat.dis-nn] [[Search INSPIRE](#)].